A&A 488, 1047–1055 (2008)
DOI: 10.1051/0004-6361:200809837

Astronomy & Astrophysics

Magnetic activity on V889 Herculis⋆,⋆⋆

Combining photometry and spectroscopy

S. P. Järvinen[1,2,3], H. Korhonen[4], S. V. Berdyugina[5,2], I. Ilyin[1], K. G. Strassmeier[1], M. Weber[1], I. Savanov[6], and I. Tuominen[7]

[1] Astrophysikalisches Institut Potsdam, An der Sternwarte 16, 14482 Potsdam, Germany
e-mail: sjarvinen@aip.de
[2] Tuorla Observatory, University of Turku, 21500 Piikkiö, Finland
[3] Astronomy Division, PO Box 3000, 90014 University of Oulu, Finland
[4] European Southern Observatory, Karl-Schwarzschild-Straße 2, 85748 Garching bei München, Germany
[5] Institute of Astronomy, ETH Zentrum, 8092 Zürich, Switzerland
[6] Armagh Observatory, College Hill, Armagh BT61 9DG, N. Ireland
[7] Observatory, PO Box 14, 00014 University of Helsinki, Finland

Received 24 March 2008 / Accepted 17 June 2008

ABSTRACT

Aims. In this paper we analyse photometric and spectroscopic observations of the young active dwarf V889 Her. We present new surface temperature maps, and compare them to earlier published Doppler maps, as well as to the results obtained from long-term photometry.
Methods. The light curve inversions and surface temperature maps were obtained using the Occamian approach inversion technique.
Results. The 12 years of photometric records on V889 Her suggest a possible photometric cycle of approximately 9 years. Variability on this time scale is detected in the maximum, minimum, and mean photometric magnitudes. The spots prefer to concentrate on two active longitudes that are approximately 180° apart. Furthermore, one flip-flop event, i.e., a sudden change of the dominant active longitude by 180°, is detected at the time of the global maximum activity. The wings of the Ca II 8662 Å indicate that the quiet photosphere of the V889 Her is similar to the one of the present Sun supporting earlier determined atmospheric parameters, while the chromosphere of V889 Her shows signs of much stronger activity. The temperature maps reveal that the polar regions are covered by spots, which are about 1500 K cooler than the quiet photosphere. The mean spot latitude varies slightly with time. It appears that the spot latitudes from our Doppler images and the spot migration rates revealed by photometry indicate a weaker differential rotation than reported earlier, but in the same (solar-like) direction.

Key words. stars: imaging – stars: activity – stars: starspots – stars: individual: V889 Her

1. Introduction

Cyclic variations in the magnetic activity in stars with spectral types from early-F to early-M on or near the main sequence were already detected in the late 70s (Wilson 1978). The survey carried out in the Ca II H & K lines at the Mount Wilson Observatory revealed three main types of variability that depend on the stellar age. Older stars tend to either vary in a smooth, cyclic fashion or have steady levels of the H & K emission. Young, active stars vary strongly but irregularly. Later, it was also noticed that on a year-to-year time scale, young active stars become fainter when their Ca II emission increases, while older less active stars – like the Sun – become brighter (e.g., Radick et al. 1998; Lockwood et al. 2007). This has generally been interpreted as a change from spot-dominated to faculae-dominated activity with stellar age.

Despite the irregular Ca II emission variations, some young solar analogues are known to show photometric cycles analogous to the 11-yr solar spot cycle but with larger amplitudes (Berdyugina et al. 2002; Berdyugina & Järvinen 2005). One of them, the Sun-like G1.5 young dwarf EK Dra, has a cycle length similar to the sunspot cycle, although with a long-term increasing trend of activity (Järvinen et al. 2005). Unfortunately, in many cases, the photometric records are still not long enough for a reliable cycle length estimate. Large amplitude photometric variations imply larger starspots (or possibly groups of smaller spots) than are seen on the Sun. Such stars are therefore suited to Doppler imaging. However, up to now there usually are only a couple of Doppler maps for young solar proxies, and there has not been a systematic study of the starspot evolution during a cycle.

V889 Her (HD 171488) is a young, apparently single, rapidly rotating, solar type G0 V dwarf. The projected rotational velocity $v \sin i$ has been measured ranging from 33 km s^{-1} (Henry et al. 1995) to 45 km s^{-1} (Cutispoto et al. 2002). Surface structure maps obtained with Doppler imaging techniques exist for two epochs: 1998 and 2004 (Strassmeier et al. 2003; Marsden et al. 2006, respectively). In both cases, a prominent polar spot and marginally resolved lower latitude features were recovered.

⋆ Based on observations made with the Nordic Optical Telescope, operated on the island of La Palma jointly by Denmark, Finland, Iceland, Norway, and Sweden, in the Spanish Observatorio del Roque de los Muchachos of the Instituto de Astrofisica de Canarias.
⋆⋆ Table 1 and Figs. 7–11 are only available in electronic form at http://www.aanda.org

In the present paper, we study the spot patterns on V889 Her at different times during the activity cycle. In the analysis new spectroscopic and photometric data are used. Observations and reduction procedures are described in Sect. 2. In Sect. 3 we explain the light curve inversion method and present results obtained using it. The Doppler imaging technique and results are described in Sect. 4, and the results are further discussed in Sect. 5. Finally, we summarise our findings in Sect. 6.

2. Observations and data reduction

2.1. Photometry

To search for long-lived spot structures and activity cycles, we collected the available photometry and compiled a data set covering 12 years from the mid 1995 to the mid 2007 (Fig. 1). The V-band was chosen for the analysis since it presents the most complete data set. Also, this band gives the maximum flux for the solar type stars and it, or any other redder band, reflects well the temperature variations that are caused by cool spots. Moreover, flares are seen in U and B-band observations, but the V-band is rather insensitive to them. Additionally, also some Strömgren y-band data have been used, after it has been transformed into Johnson V magnitudes as described by Olsen (1984). The earliest 1995 Johnson V magnitudes are published by Cutispoto et al. (1999). The rest of the data until 2003 were presented earlier by Strassmeier et al. (2003). These are mostly Johnson V magnitudes, but some of the 1997–1998 observations are Strömgren y magnitudes.

The new data presented in this paper, starting from 2003, were taken with the Amadeus 0.75 m automatic photoelectric telescope of the University of Vienna at the Fairborn Observatory in southern Arizona. Amadeus is optimised for red wavelengths with an EMI-9828 tube and Johnson-Cousins $V(I_C)$ filters (for more details see Strassmeier et al. 1997b). Measurements were made differentially between the variable, a comparison star (HD 171286), a check star (HD 170829), and the sky position. The data reduction is also automatic and was described by Strassmeier et al. (1997a) and Granzer et al. (2001).

The data were divided into 20 sets, so that most of the sets had a good phase coverage over the rotational period and each set represented a light curve that is stable for a given time interval (Fig. 2). The individual data points show quite large scatter. This might be explained by the large stellar differential rotation reported by Marsden et al. (2006): since the overall shape of the light curve remained rather stable during months, the rotational modulation were most probably dominated by the high-latitude spot configuration, while the scatter could be caused by more rapidly rotating smaller spots closer to the equator.

The observations were phased with the ephemeris

$$T = 2\,449\,950.550 + 1^{\rm d}.33697\,E, \quad (1)$$

where the zero-phase Julian date is the time of the first photometric observation in the data set used in the current study, and the period represents the mean rotation period of spots determined from all the sets. The period used here is within the error of the period reported by Strassmeier et al. (2003), i.e., $P = 1.3371 \pm 0.0002$ days, which was determined with a period analysis based on the photometry from only one year. The first iteration of our analysis was done using this value, but over the 12-yr time interval, it caused a small, but still clearly detectable, linear trend in the spot phases. The corrected value was obtained by removing that drift. Both period values differ significantly from the one reported by Marsden et al. (2006), i.e., $P = 1.313 \pm 0.004$ days. However, this value is the inferred equatorial rotation period, while the two other values are based on the light curve modulations caused primarily by high-latitude spots.

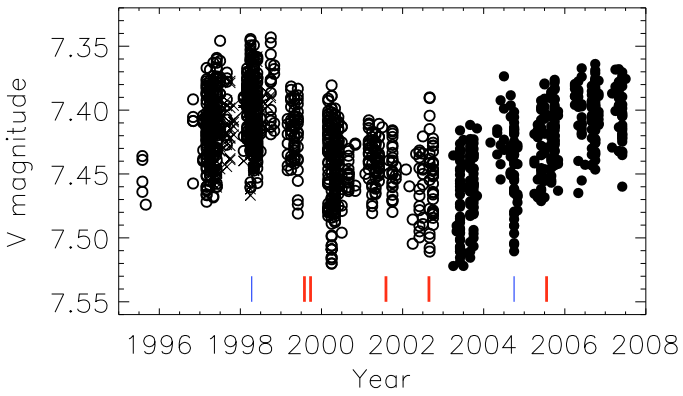

Fig. 1. The photometric data analysed in this paper. Open circles and crosses denote previously published V-band and y-band (transformed into V magnitudes) photometry, respectively, while filled circles represent the new data. The vertical ticks on the bottom of the plot denote epochs of obtained Doppler maps. Thin (blue) ticks mark earlier published maps and thick (red) ticks identify maps presented in this paper.

2.2. Spectroscopy

Spectroscopic observations of V889 Her were carried out with the Nordic Optical Telescope (NOT, La Palma) using the SOFIN échelle spectrograph during six observing runs: July/August 1999, September 1999, October 1999, July/August 2001, August 2002, and July 2005. The data were acquired with the 2nd camera, which provided 33 useful orders in the spectral range of 3930–9040 Å. With the slit width of 81 μm for the first four runs and 65 μm for the last two, the observations have the resolution ($\lambda/\Delta\lambda$) of about 77 000, and the spectra are centred at 6430–6440 Å. More information is presented in Table 1, which is only available in electronic form.

The spectra were reduced with the 4A software package (Ilyin 2000). The reduction included bias subtraction, an estimate of the variance of the flux, master flat-field correction, scattered light subtraction with the aid of 2D-smoothing splines, spectral order definition, and weighted integration of the flux with cosmic spike elimination. The wavelength calibration was obtained using Th–Ar comparison spectra.

3. Light curve inversions

3.1. The inversion technique

To determine locations of spots on the stellar surface, we performed inversions of the phased light curves into stellar images using the Occamian inversion technique (Berdyugina 1998; Berdyugina et al. 2002). The model assumes that, due to the low spatial resolution, the local intensity of the stellar surface always contains contributions from the photosphere and from cool spots weighted by the fraction of the surface covered by spots, i.e., the spot filling factor f_s. The inversion of a light curve results in a distribution of the spot filling factor over the visible stellar surface. Since a light curve represents a one-dimensional time series, the resulting stellar image contains information mostly in the direction of rotation, i.e., in the longitude, while

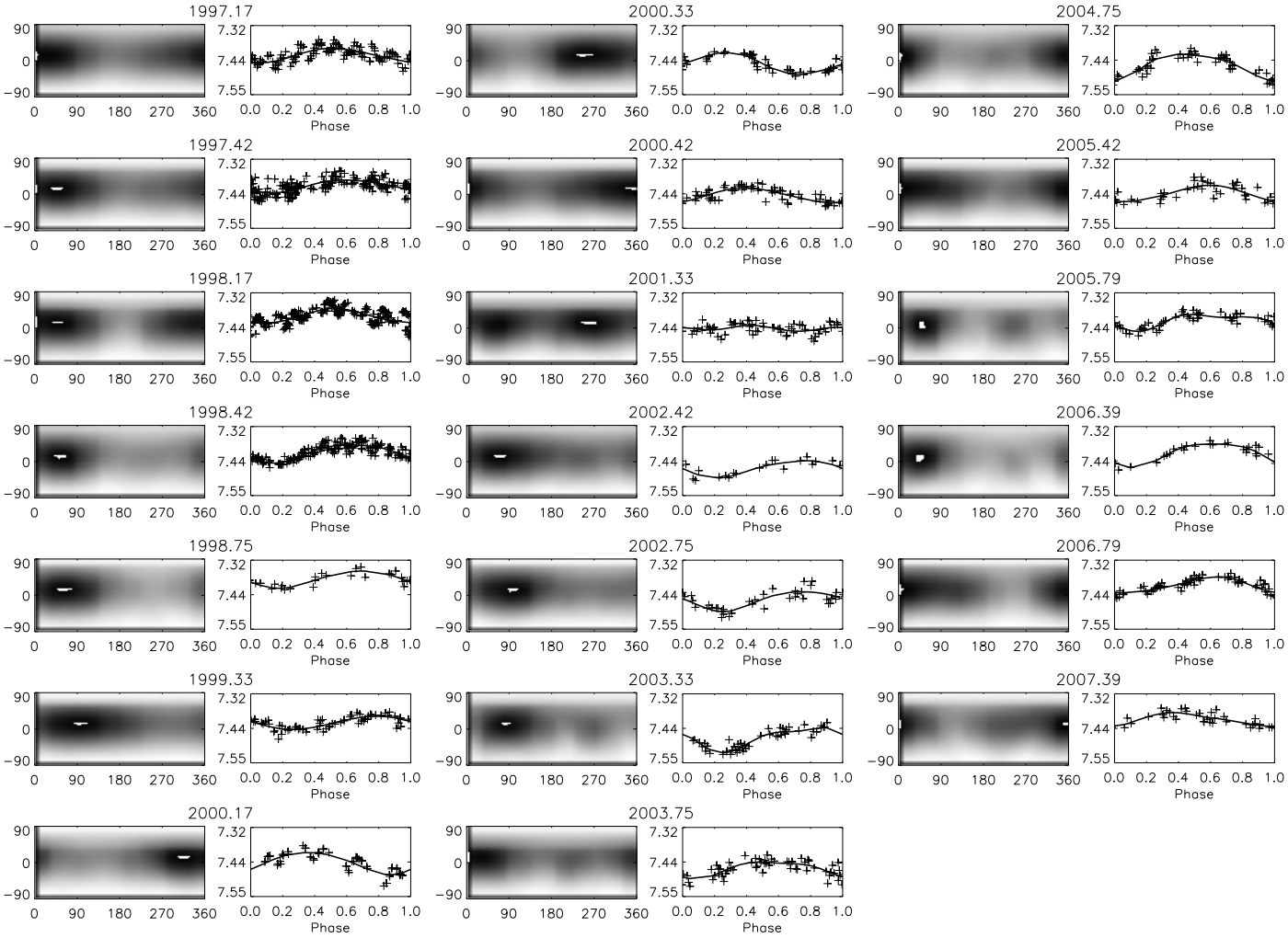

Fig. 2. The light curve inversion results are shown in the left columns. The spot filling factor is larger in the darker regions with maximum value highlighted in white. In the right column observed and calculated V-band light curves are presented by crosses and lines, respectively.

the spot size and locations in the latitude remain comparably ill-determined. Examples from an independent numerical parameter study have been presented recently by Savanov & Strassmeier (2008), which showed the strengths and limitations of such inversions. However, because of the projection effects and limb darkening, the inversion technique can recover more structure than is obvious at first glance from the shape of the light curve, and is very useful for determining longitudes of spot concentrations. Although this approach is less informative than the Doppler imaging technique, the analysis of long series of photometric observations allows us to recover longitudinal spot patterns and study their long-term evolution.

For V889 Her, values of the photospheric and spot temperatures were assumed to be 5800 K and 4200 K, respectively (Strassmeier et al. 2003). However, since we were only interested in the spot longitudes, possible errors in the temperature values were not important. For the inversions, the stellar surface was divided into a grid of 10° × 10°, and the f_s values were determined for each grid pixel. The recovered stellar pseudo images and fits to the observed light curves are shown in Fig. 2. Usually the spot filling factor maps of V889 Her reveal only one spot concentration on the entire stellar surface. For some epochs, traces of a secondary concentration are also seen.

3.2. Active longitudes and flip-flops

The spot maps in Fig. 2 indicate rather asymmetrically distributed spot filling factors across the stellar surface. The pixels that have the highest spot filling factors are marked with a bright dot for better visibility. Longitudes of the maximum f_s values were recovered from the images (also dubbed spot phases). Obviously, their accuracy is limited by the large width of the light curve minima. The numerical values are given in Table 2. The time dependence of the spot phases is shown in Fig. 3a for the phase interval 0.0 to 1.0 and in Fig. 3b for a continuous phase range with the measurements repeated by adding or subtracting an integer number corresponding to the number of full stellar rotations. The latter is done to reveal a possible long-term migration of the active regions (e.g., Panov & Dimitrov 2007).

It is clear that before the global photometric minimum in 2002 spots migrated towards larger phases, with the rate ~0.15 yr^{-1}, and after that towards earlier phases, with the rate ~0.06 yr^{-1}. These correspond to average spot rotation periods of 1.3377 days and 1.3367 days, respectively. Interestingly, the two opposite migration rates occurred during the years when the overall activity level of the star was correspondingly increasing (before 2002) and decreasing (after 2002, see Fig. 1). Since the

Table 2. Spot parameters from photometric inversions: HJD is the heliocentric Julian date −2 400 000 at the beginning and at the end of data set and φ is the recovered phase of the active region 1 and 2, respectively.

Set	Year	HJD (beg)	HJD (end)	φ_1	φ_2
1	1997.17	50 498	50 565	0.069	–
2	1997.42	50 566	50 637	0.153	–
3	1998.17	50 868	50 939	0.125	0.750
4	1998.42	50 942	50 997	0.153	–
5	1998.75	51 077	51 126	0.181	–
6	1999.33	51 247	51 360	0.264	–
7	2000.17	51 605	51 645	0.875	–
8	2000.33	51 672	51 692	0.681	–
9	2000.42	51 685	51 712	0.958	0.681
10	2001.33	51 976	52 093	0.708	0.181
11	2002.42	52 416	52 463	0.181	0.625
12	2002.75	52 534	52 578	0.264	–
13	2003.33	52 751	52 831	0.236	0.736
14	2003.75	52 896	52 949	0.097	0.625
15	2004.75	53 280	53 321	0.014	0.597
16	2005.42	53 480	53 568	0.014	0.319
17	2005.79	53 628	53 687	0.153	0.653
18	2006.39	53 833	53 923	0.125	0.625
19	2006.79	53 997	54 054	0.014	0.375
20	2007.39	54 207	54 283	−0.014	0.681

migration is seen with respect to the reference frame rotating with the fixed averaged period (Eq. (1)), it therefore likely indicates different rotation periods of active regions during different phases of the stellar activity cycle, i.e., reveals the differential rotation and implies that spots occupied different latitudes before and after the year 2002. Our Doppler imaging results support this conclusion (see Sect. 4).

The spots on V889 Her were concentrated mainly in one of the two active longitudes about 180° ($\Delta\varphi = 0.5$) apart. When the dominant spot concentration switches to another active longitude, we may observe this as a so-called flip-flop. This effect was first detected in FK Com (Jetsu et al. 1991, 1993). Later it was found to be cyclic in RS CVn- and FK Com-type stars, as well as in some young solar analogues (e.g., Berdyugina & Tuominen 1998; Rodonò et al. 2000; Korhonen et al. 2002; Berdyugina & Järvinen 2005).

One can see in Fig. 3 that primary spots change clearly from one active longitude to another, indicating the presence of a flip-flop effect: before 2002 the larger region was on one active longitude and after that on the opposite one. The moment of the flip-flop event coincides with the overall all-time photometric minimum observed for this star in 2002–2003. Similar behaviour was found for the rapidly-rotating K subgiant V1355 Ori, where Savanov & Strassmeier (2008) detected a periodic flip-flop that always coincided with minimum system light and with minimum spot amplitude, i.e., maximum spottedness. Since the change from one active longitude to another is detected only once for V889 Her, it is not possible to say whether this phenomenon is cyclic in our case. If it later turned out to be cyclic, the present data would already indicate a longer cycle than any detected in other solar proxies.

4. Doppler imaging

4.1. Line profiles and inversions

Three atomic lines were selected for Doppler imaging: Fe I 6411.64 Å, Fe I 6430.80 Å, and Ca I 6439.08 Å. Local line profiles were calculated with the code by Berdyugina (1991), which includes calculations of opacities in the continuum and in the atomic and molecular lines, although molecular lines were omitted here, since they do not contribute to the spectrum of V889 Her at chosen wavelengths. Atomic line parameters for a given wavelength region were obtained from Vienna Atomic Line Database (VALD) for lines having a central depth of 1% or more (e.g., Piskunov et al. 1995; Kupka et al. 1999). The stellar model atmospheres used here are from Kurucz (1993). The local line profiles were calculated for 20 values of $\mu = \cos\theta$ from the disc centre to the limb. The spectra were calculated for temperatures ranging from 4000 K to 6500 K in steps of 250 K.

The Occamian approach was used for inversions of the observed line profiles into stellar images (Berdyugina 1998). A $6° \times 6°$ grid on the stellar surface was used for integrating local line profiles into normalised flux profiles. With a set of stellar atmosphere models, the stellar image is considered as the distribution of the effective temperature across the stellar surface, as is usually done in surface imaging. The adopted stellar parameters are given in Table 3. Furthermore, we used solar abundances.

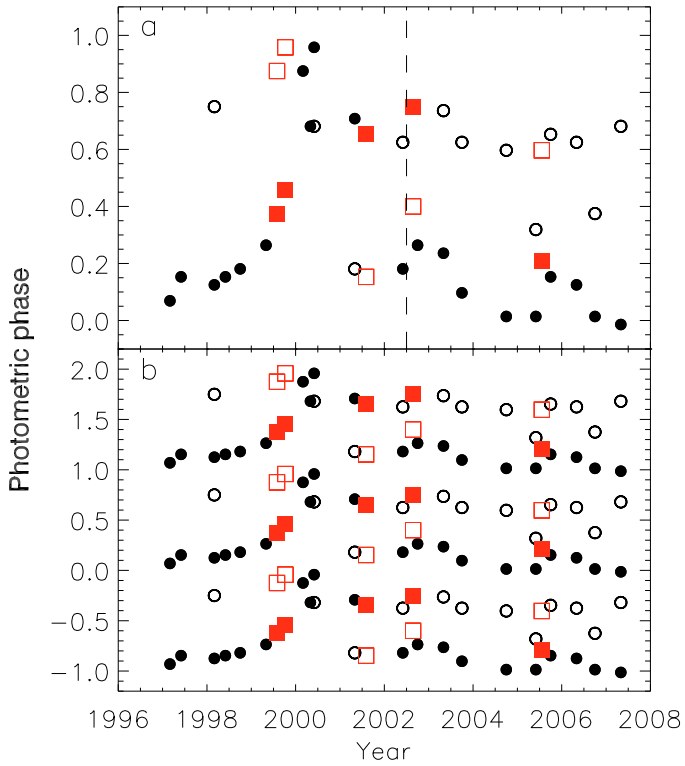

Fig. 3. a) Phases of the spots recovered on the surface of V889 Her using the light curve inversion technique. Filled circles denote the primary spot and open circles the secondary spot. Filled (red) squares denote phases of primary spots and open (red) squares phases of secondary spots determined from the Doppler maps obtained in this paper (see Sect. 4). The flip-flop event is marked with vertical dashed line. **b)** Multiple phase plot to study possible spot migration.

4.2. Temperature maps

The surface temperature maps of V889 Her for the years 1999.58, 1999.77, 2001.65, 2002.65, and 2005.55 are shown in Fig. 4. To have a sufficient phase coverage, we have combined data sets from September and October 1999 into a single 1999.77 map. We further note that in 2005.55, we have some observations taken several days apart at almost the same rotational

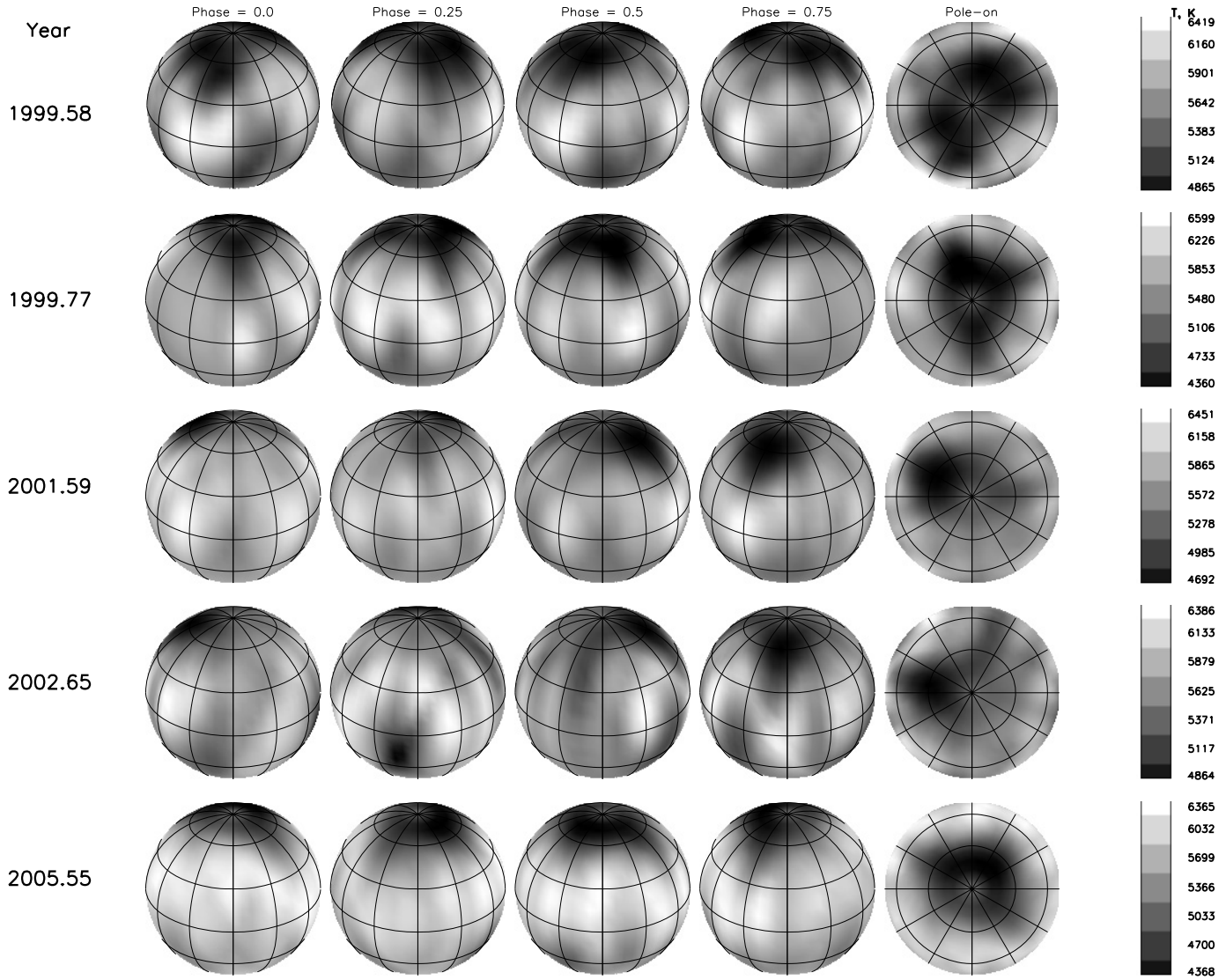

Fig. 4. The surface temperature maps of V889 Her for five epochs obtained with the Occamian approach. Note the changing temperature scale.

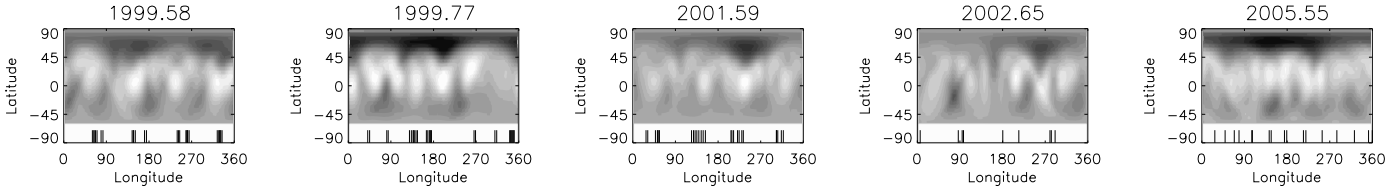

Fig. 5. The surface temperature maps from Fig. 4 shown in a Mercator projection. The phases of the spectroscopic observations are shown with vertical dashes at the bottom in the area from which we have no information due to the inclination of the star.

phase. However, the resulting map does not show any significant changes whether all the spectra are used or not. In all five cases, the spots are concentrated on high latitudes. The small hot regions near the equator seen in all the maps are most likely artifacts. If they are ignored, the unspotted photospheric temperature is about 5900 K. A similar value has already been determined earlier by Strassmeier et al. (2003). The high-latitude spots are 1400–1600 K cooler than the unspotted stellar surface, which also agrees with the temperature determined for the polar spot seen in the 1998 April map (Strassmeier et al. 2003). Also spots with less contrast (ΔT ≈500–1000 K) are seen.

The first two maps show two active high-latitude regions located roughly 180° apart. The two subsequent maps show a clear spot concentration on just one side of the star centred around latitude +60°. In the last map the spots are more compactly concentrated forming an antisymmetric polar spot. The last map is very similar to the one of Marsden et al. (2006), obtained almost one year earlier. The primary feature is even above a latitude +60°, although in their map it was also almost pole-symmetric, while the low-latitude features were more concentrated on one side. We emphasise that the phase coverage for our last image is the best of all our maps but that the very low-latitude features (below, say, −20°) are still artifacts due to imperfect phase coverage and the well-known mirroring effect in Doppler imaging (e.g., Rice 2002).

The longitudes at which the spectroscopic observations were taken are shown at the bottom of the Mercator projections of the temperature maps (Fig. 5), within the area from which we have

Table 3. Stellar parameters of V889 Her.

Parameter	Value
P, days	1.33697
$T_{\rm eff}$, K	5830 ± 50
$\log g$	4.5
$\xi_{\rm t}$, km s^{-1}	1.6 ± 0.1
$\zeta_{\rm t}$, km s^{-1}	3.0
$v \sin i$, km s^{-1}	37.5 ± 0.5
Inclination, i	$60° \pm 10°$

Note: The effective temperature, surface gravity and macroturbulence are from Strassmeier et al. (2003). The $v \sin i$ and inclination are adopted from Marsden et al. (2006). The given microturbulence value is from this work.

no information due to the inclination of the star. Representative fits to the observed spectra are illustrated in Fig. 6 for all the three lines used in the inversions. Figures 7–11 (available in electronic form only) show fits to all of the phases for all data sets.

5. Discussion

5.1. Spot latitudes

The top panel of Fig. 12 shows the latitudinal spot distributions at different times. For all the maps, one temperature value (5150 K) was assumed to separate between spotted and unspotted photosphere. The value has been chosen so that also penumbra-like structures, if present, are included. However, from the Sun we know that the temperature structure in the penumbra depends on the feature and height: the coolest dark filaments are about 750 K below the unspotted surface temperature, while the temperature difference in the case of the bright filaments is only about 250 K below. A slightly lower temperature was chosen to include also unresolved small spots, which are on average cooler than the penumbra.

When looking at the whole longitude range, one can see that the spots are constantly located at high latitudes covering the polar region up to 85°. Note that no information at exactly 90° can be retrieved with Doppler imaging due to the missing Doppler information. The extensions toward lower latitudes never reach below +35°. The mean spot latitude changes about 5° between the first and the last map and the largest mean latitude difference (almost 10°) is between the last maps, the spots being at higher latitudes in the last map. Similarly, the spots shift towards higher latitudes between the first and the second map. Thus, the spot mean latitude was lowest (~60°) at the time of the global photometric minimum (activity maximum), occurring in 2002–2003, and increased at times of lower activity. This may indicate the existence of a solar-like latitude drift ("Spörer's law") on V889 Her.

We were also interested in seeing whether the spots have different mean latitudes around the opposite active longitudes. We consider here an active longitude as a stellar hemisphere centred on a given spot concentration recovered from the photometric data, the first one corresponding to the lower active longitude in Fig. 3 (near phase 0.0 in the years 1997–1998) and the second one 180° apart. The latitudes covered by spots within such active longitudes are shown in the middle and bottom panel of Fig. 12. One can see that before 2002 spots within the first active longitude were on average at lower latitudes than the ones within the second active longitude, while after 2002 the situation changed to the opposite. A similar behaviour was also found on the very active RS CVn-type star HR 1099 (Berdyugina & Henry 2007) and on a young solar analogue EK Dra (Järvinen et al. 2007).

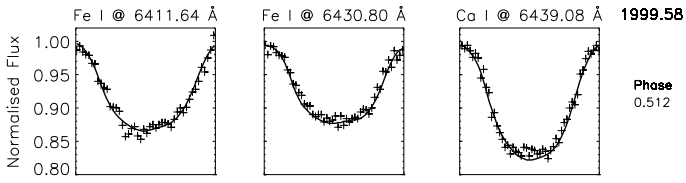

Fig. 6. Example of calculated (solid curves) and observed (crosses) spectral line profiles for one phase in the 1999.58 data set.

5.2. Differential rotation and solar-type activity cycle

Marsden et al. (2006) reported that V889 Her shows solar-type surface differential rotation with $\Omega_{\rm eq} = 4.786$ rad/day and $\Delta\Omega = 0.402$ rad/day, i.e., with more rapid rotation at lower latitudes. They estimated that the equator of the star laps the poles every $\sim 16 \pm 2$ d and, thus, has a photospheric differential rotation approximately seven times the solar value. As already mentioned in Sect. 3.2, the migration of the phases of the spots seen in Fig. 3 reveals the differential rotation as well. The surface temperature maps show that the spot concentration appears at lowest latitudes (~60°) at the time of the global photometric minimum around 2002, when the rotation period was also the shortest. This supports the solar-type differential rotation. However, the period for the latitude 60° based on the parameters obtained by Marsden et al. (2006) appears much longer (~1.40 days) than detected by us from spot migration. It appears that the spot latitudes revealed in our Doppler images and the spot migration rates revealed by photometry indicate a weaker differential rotation than reported by Marsden et al. (2006).

The length of the spot cycle on V889 Her is estimated from the subsets of the photometric data record presented in Fig. 1 using the Lomb method for unevenly sampled data (Press et al. 1992). Since the current record covers only one cycle, more data is clearly needed to confirm whether the overall brightness of the star really varies periodically and, if so, maybe with more than just a single cycle period as found for many other active stars (Oláh et al. 2007). The maximum, mean, and minimum magnitudes of each sub light curve indicate a variation with an approximately 9 ± 2 year period (false alarm probability 3×10^{-2}, 8×10^{-3}, and 4×10^{-2}, respectively). Amplitude variations indicated a 5.9 ± 0.7 year period. If this period is related to a possible flip-flop cycle, as in some other young solar proxies, we may expect the next flip-flop to take place around the year 2008.

5.3. Comparing photometric and spectroscopic spot phases

The phases of the spots obtained from the temperature maps are overplotted on top of the phases determined from the photometric inversions (Fig. 3). In general, the phases obtained from Doppler images agree well with the photometric results.

The phases of the spots from the two first maps show some deviation from the general trend, but that can be explained by a migration of the active regions. In the 2002.65 map the primary and secondary spots are at the expected phases but their relative sizes disagree with the photometric data. This may be due to an insufficient phase coverage of the Doppler map which is the poorest in our sample. The low-latitude spot near the phase 0.2 might be responsible for the photometric modulation, but its size and latitude could not be well-constrained by the data. It is

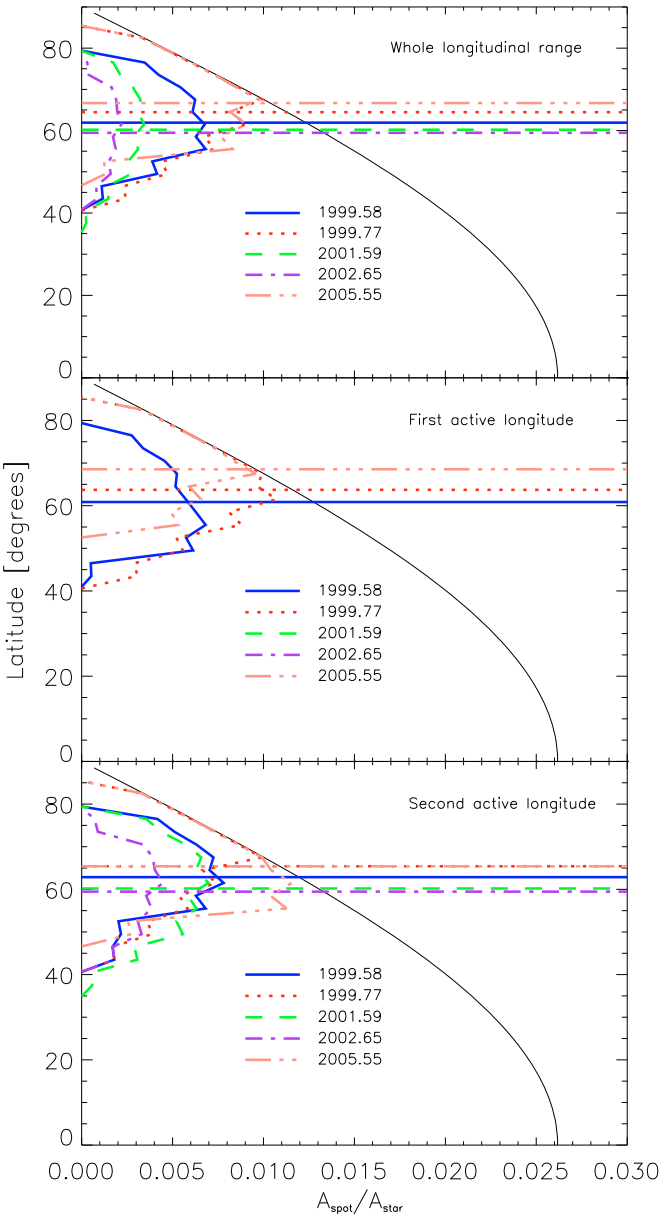

Fig. 12. The latitudinal distribution of the spots recovered in the five surface maps (thick lines). The thin solid curve denotes the fraction of the stellar surface within each latitude, and the horizontal lines mark the mid latitude of the spots. Both active longitudes have a width of 180°. *Top panel*: the whole longitudinal range. *Middle panel*: around the first active longitude, which is the half of the star centred at given time at the lower (first) active longitude in Fig. 3. *Bottom panel*: around the second active longitude which is the half of the star centred at given time to upper (second) active longitude in Fig. 3.

interesting, however, that this map is obtained close to the time of the flip-flop and indicates the presence of spots on both active longitudes on opposite stellar hemispheres.

5.4. The chromospheric activity

The infrared triplet lines of ionised calcium (Ca II IRT) at 8489, 8542, and 8662 Å are prominent features in the spectra of late-type stars. Their extended wings probe a wide range of photospheric layers and are sensitive to the temperature distribution in the atmosphere of the star (Andretta et al. 2005). Their cores are formed in the chromosphere and, hence, central depressions are sensitive to the degree of activity in outer layers.

In August and September 1993, Mulliss & Bopp (1994) observed Hα and the Ca II IRT-2 line at 8542 Å in 10 stars, including V889 Her. They reported emission reversals in both the Hα and IRT-2 lines. More recently, in February 2002, Busà et al. (2007) observed 42 stars, covering the whole IRT range. In V889 Her, the residual equivalent width was smallest for the IRT-1 line, while the IRT-2 line shows the most prominent emission reversal. The emission reversal was also detected in the IRT-3 line with an equivalent width of 510.7 ± 142.8 mÅ, but it was clearly weaker than in the IRT-2. Since 2001 our observations have covered the IRT-3 line (8662 Å), and we clearly see the emission reversal as visualised in Fig. 13.

Furthermore, the rotationally broadened solar profile matches the wings of the average Ca II IRT-3 line profile of V889 Her very closely, which implies that the thermodynamic structure of the quiet photospheres of the two stars is very similar. On the other hand, the emission reversal indicates that the chromospheres are different.

For a more detailed analysis of the emission reversal profiles, we subtracted the broadened solar profile from the observed profiles. Figure 14 shows variations in the Ca II IRT-3 line emission reversal equivalent width (W_λ) measured from the three latest data sets, and the shapes of the synthetic light curves calculated from the corresponding temperature maps. The measured equivalent widths are smaller but within the errors for IRT-3 line emission reversal equivalent width reported by Busà et al. (2007). The 2002.65 data set gives the smallest and 2005.55 data set the largest equivalent widths. This is consistent with the spot coverage being smallest in 2002.65 map and largest in 2005.55 map.

The 2001.59 data set gives a rather flat distribution of W_λ with some scatter and large error bars. However, although there is a gap in spectral observations at the minimum ($\varphi = 0.65$) of the calculated light curve, up to an 11% increase in W_λ is detected in surrounding points. In the 2002.65 data set the largest equivalent width is probably caused by a flare event. Here the distribution of phases is poor, but the W_λ is larger by 20% at the light curve minimum around $\varphi = 0.75$. Also in the 2005.55 data set, the largest W_λ is probably due to a flare event. The two other larger widths correlate spatially width a secondary minimum ($\varphi = 0.65$) seen in the calculated light curve. The distribution of the phases in spectral observations is very good in this case and a nice anti-correlation between equivalent widths and calculated light curve is seen. At both the primary ($\varphi = 0.22$) and secondary ($\varphi = 0.65$) light curve minima a 15% increase occurs in the equivalent width.

In conclusion, since the emission reversal is detected in all observed spectra and the measured W_λ never reaches zero, this indicates that there is always some fraction of the chromosphere covered with plages, as well as some fraction of the photosphere covered with spots.

6. Summary

From the photometric and spectroscopic study of V889 Her, the following results have been obtained:

1. The maximum, mean, and minimum magnitudes vary possibly in a ~9 year period. Variations in the light curve amplitude indicate a 5.9 year change.

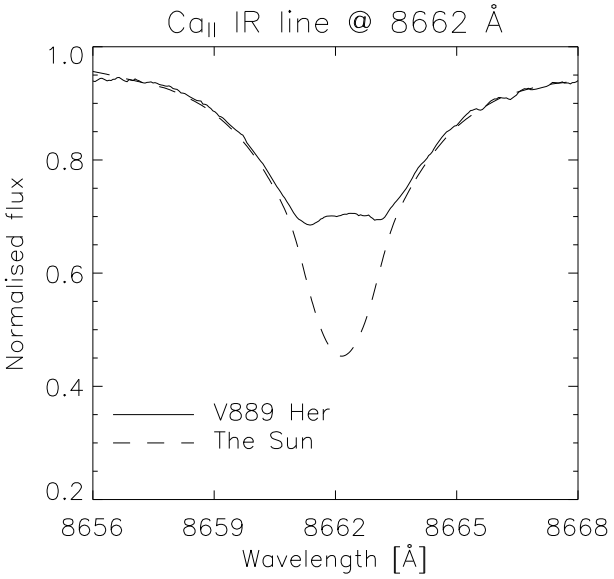

Fig. 13. The average profile of all Ca II IRT-3 lines (solid line), together with the rotationally broadened observed solar profile (dashed line).

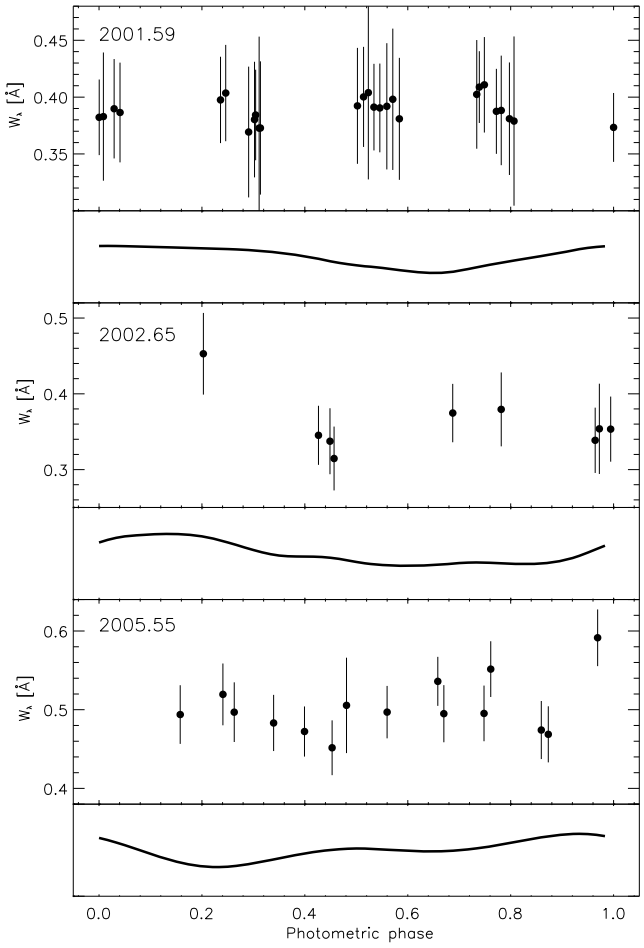

Fig. 14. The variation of the Ca II IRT-3 line emission reversal equivalent width (W_λ) marked as dots from the three latest observing runs. For comparison under the data sets the shape of the light curve calculated from the temperature maps is shown with a solid line.

2. The spots on surface of V889 Her are grouped around two active longitudes on average 180° apart. Their centres are found to drift in the fixed reference frame due to differential rotation as in other solar analogues.
3. The dominant activity changed to the opposite longitude after 2002, indicating a flip-flop event. The current photometric record is not long enough to conclude on a flip-flop cycle, but if it exists, the cycle length would be longer than detected in other young solar analogues.
4. Excellent agreement between the V889 Her Ca II IRT-3 line and the rotationally broadened solar profile in the line wings implies that both stars have comparable photospheres, thus supporting the adopted atmosphere parameters. However, an emission reversal detected in the Ca II IRT-3 line implies that the chromosphere of V889 Her is more active than the Sun's and is constantly covered by plages.
5. The five temperature maps obtained by inversions of atomic line profiles show very high-latitude spots of about 1500 K cooler than the quiet photosphere. The near-pole region seems to be constantly covered with spots, which sometimes have extensions toward the lower latitudes.
6. The spot phases determined from the temperature maps are in good agreement with the phases determined from the photometric inversions.
7. The mean spot latitudes were lowest (~60°) at the time of the global photometric minimum (activity maximum) in 2002 and 5°–10° higher at the adjacent epochs.
8. The long-term spot migration combined with the mean spot latitudes indicates a solar-type differential rotation but substantially weaker than that reported by Marsden et al. (2006).
9. The equivalent width of the emission in the Ca II IRT-3 line increases ~10–20% at the light curve minimum.

Acknowledgements. S.P.J., H.K. & K.G.S. acknowledge the support by the Deutsche Forschungsgemeinschaft, grant KO 2320/1-2. S.V.B. acknowledges the EURYI Award from the European Science Foundation (`http://www.esf.org/euryi`) and the SNF grant PE002-104552.

References

Andretta, V., Busà, I., Gomez, M.T., & Terranegra, L. 2005, A&A, 430, 669
Berdyugina, S. V. 1991, Izv. Krymsk. Astrofiz. Obs., 83, 102
Berdyugina, S. V. 1998, A&A, 338, 97
Berdyugina, S. V., & Henry, G.W. 2007, ApJ, 659, L157
Berdyugina, S. V., & Järvinen, S.P. 2005, AN, 326, 283
Berdyugina, S. V., & Tuominen, I. 1998, A&A, 336, L25
Berdyugina, S. V., Pelt, J., & Tuominen, I. 2002, A&A, 394, 505
Busà, I., Aznar Cuadrado, R., Terranegra, L., Andretta, V., & Gomez, M.T. 2007, A&A, 466, 1089
Cutispoto, G., Pastori, L., Tagliaferri, G., Messina, S., & Pallavicini, R. 1999, A&AS, 138, 87
Cutispoto, G., Pastori, L., Pasquini, L., et al. 2002, A&A, 384, 491
Granzer, T., Reegen, P., & Strassmeier, K. G. 2001, AN, 322, 325
Henry, G. W., Fekel, F. C., & Hall, D. S. 1995, AJ, 110, 2926
Ilyin, I. 2000, Ph.D. Thesis, University of Oulu, Finland
Järvinen, S. P., Berdyugina, S. V., & Strassmeier, K. G. 2005, A&A, 440, 735
Järvinen, S. P., Berdyugina, S. V., Korhonen, H., Ilyin, I., & Tuominen, I. 2007, A&A, 472, 887
Jetsu, L., Pelt, J., Tuominen, I., & Nations, H. 1991, in The Sun and Cool Stars: activity, magnetism, dynamos, ed. I. Tuominen, D. Moss, & G. Rüdiger, (Berlin: Springer), Proc. IAU Coll., 130 381
Jetsu, L., Pelt, J., & Tuominen, I. 1993, A&A, 278, 449
Korhonen, H., Berdyugina, S. V., & Tuominen, I. 2002, A&A, 390, 179
Kupka, F., Piskunov, N. E., Ryabchikova, T. A., Stempels, H. C., & Weiss, W. W. 1999, A&AS, 138, 119
Kurucz, R. L. 1993, Kurucz CD No. 13

Lockwood, G. W., Skiff, B. A., Henry, G. W., et al. 2007, ApJS, 171, 260
Marsden, S. C., Donati, J. -F., Semel, M., Petit, P., & Carter, B.D. 2006, MNRAS, 370, 468
Mulliss, C. L., & Bopp, B. W. 1994, PASP, 106, 822
Oláh, K., Strassmeier, K. G., Granzer, T., Soon, W., & Baliunas, S.L. 2007, AN, 328, 1072
Olsen, E. H. 1984, A&AS, 57, 443
Panov, K., & Dimitrov, D. 2007, A&A, 467, 229
Piskunov, N. E., Kupka, F., Ryabchikova, T. A., Weiss, W. W., & Jeffery, C. S. 1995, A&AS, 112, 525
Press, W. H., Teukolsky, S. A., Vetterling, W. T., & Flannery, B.P. 1992, in Numerical Recipes in FORTRAN – The Art of Scientific Computing, second edition (New York, USA: Cambridge University Press), 569
Radick, R. R., Lockwood, G. W., Skiff, B.A., & Baliunas, S.L. 1998, ApJS, 118, 239
Rice, J. B. 2002, AN, 323, 220
Rodonò, M., Messina, S., Lanza, L.F., Cutispoto, G., & Teriaca, L. 2000, A&A, 358, 624
Savanov, I. S., & Strassmeier, K. G. 2008, AN, 329, 364
Schlegel, D. J., Finkbeiner, D. P., & Davis, M. 1998, ApJ, 500, 525
Strassmeier, K. G., Bartus, J., Cutispoto, G., & Rodonò, M. 1997a, A&AS, 125, 11
Strassmeier, K. G., Boyd, L. J., Epand, D. H., & Granzer T. 1997b, PASP, 109, 697
Strassmeier, K. G., Pichler, T., Weber, M., & Granzer, T. 2003, A&A, 411, 595
Wilson, O. C. 1978, ApJ, 226, 379

Table 1. The spectroscopic observations of V889 Her.

HJD 2 450 000+	Day	Phase	S/N	Exp. t min	HJD 2 450 000+	Day	Phase	S/N	Exp. t min
	1999.58				1475.352698	23/10/1999	0.49133	158	17
1383.473509	23/07/1999	0.76938	181	15		*2001.59*			
1383.483806	23/07/1999	0.77708	155	12	2120.452287	29/07/2001	0.99998	216	20
1383.493261	23/07/1999	0.78415	148	13	2121.440416	30/07/2001	0.73906	235	20
1384.457167	24/07/1999	0.50512	133	10	2121.453514	30/07/2001	0.74886	180	12
1384.466800	24/07/1999	0.51232	157	15	2122.460703	31/07/2001	0.50220	152	20
1385.482655	25/07/1999	0.27214	182	16	2122.476575	31/07/2001	0.51407	158	20
1385.494366	25/07/1999	0.28090	174	15	2122.488978	31/07/2001	0.52335	94	10
1387.555687	28/07/1999	0.82269	151	15	2123.533091	02/08/2001	0.30430	183	20
1387.567028	28/07/1999	0.83117	129	15	2123.545497	02/08/2001	0.31358	123	10
1387.578383	28/07/1999	0.83966	134	15	2124.463608	02/08/2001	0.00029	181	20
1388.565836	29/07/1999	0.57824	139	20	2124.474468	02/08/2001	0.00841	124	07
1388.580679	29/07/1999	0.58934	137	20	2125.495679	03/08/2001	0.77224	198	20
1389.562286	30/07/1999	0.32354	147	20	2125.508266	04/08/2001	0.78165	166	12
1389.577131	30/07/1999	0.33465	152	20	2126.548013	05/08/2001	0.55934	133	20
1390.473483	30/07/1999	0.00508	146	15	2126.563371	05/08/2001	0.57083	120	20
1390.484859	30/07/1999	0.01359	149	15	2126.580463	05/08/2001	0.58361	135	25
1390.496234	30/07/1999	0.02210	139	15	2127.525860	06/08/2001	0.29073	134	20
1391.566258	01/08/1999	0.82243	178	15	2127.541244	06/08/2001	0.30224	124	20
1391.577622	01/08/1999	0.83093	196	15	2127.553242	06/08/2001	0.31121	87	10
1392.491905	01/08/1999	0.51478	163	15	2128.513368	07/08/2001	0.02935	176	20
1392.504902	01/08/1999	0.52450	179	20	2128.528732	07/08/2001	0.04084	155	20
1393.518918	03/08/1999	0.28294	170	15	2129.455510	07/08/2001	0.73403	160	18
1393.530298	03/08/1999	0.29146	145	15	2129.540470	08/08/2001	0.79758	164	20
1393.541672	03/08/1999	0.29996	152	15	2129.552385	08/08/2001	0.80649	113	10
1394.501487	03/08/1999	0.01787	186	15	2130.525322	09/08/2001	0.53421	181	20
1394.512866	04/08/1999	0.02638	189	15	2130.540680	09/08/2001	0.54570	188	20
1394.522508	04/08/1999	0.03359	149	10	2131.463681	09/08/2001	0.23606	179	20
	1999.73				2131.477322	09/08/2001	0.24627	160	15
1443.394330	21/09/1999	0.58775	161	15		*2002.65*			
1443.405701	21/09/1999	0.59626	170	15	2507.447328	20/08/2002	0.45677	217	15
1444.392650	22/09/1999	0.33446	191	15	2508.444642	21/08/2002	0.20272	193	13
1444.403458	22/09/1999	0.34254	157	15	2509.502938	22/08/2002	0.99428	217	20
1445.363685	23/09/1999	0.06075	143	15	2510.555518	24/08/2002	0.78157	217	15
1445.375054	23/09/1999	0.06926	119	15	2511.447671	24/08/2002	0.44887	232	20
1445.387920	23/09/1999	0.07888	138	16	2513.473523	26/08/2002	0.96412	258	20
1446.413912	24/09/1999	0.84628	62	15	2513.484448	26/08/2002	0.97229	150	07
1446.425801	24/09/1999	0.85517	29	16	2514.440571	27/08/2002	0.68744	248	20
1447.377332	25/09/1999	0.56688	98	15	2515.428592	28/08/2002	0.42644	243	17
1447.388702	25/09/1999	0.57538	93	15		*2005.55*			
1447.400069	25/09/1999	0.58389	89	15	3567.405076	15/07/2005	0.26270	267	28
1447.411445	25/09/1999	0.59240	87	15	3567.587754	16/07/2005	0.39934	324	30
1449.367666	27/09/1999	0.05557	122	17	3567.659421	16/07/2005	0.45294	240	15
1449.380151	27/09/1999	0.06491	96	16	3568.463993	16/07/2005	0.05473	298	32
1449.391857	27/09/1999	0.07366	105	15	3568.601784	17/07/2005	0.15779	300	25
1449.403235	27/09/1999	0.08217	110	15	3569.408539	17/07/2005	0.76121	295	21
	1999.81				3569.558080	18/07/2005	0.87306	245	15
1471.342771	19/10/1999	0.49207	115	14	3569.686268	18/07/2005	0.96894	217	15
1471.353450	19/10/1999	0.50006	134	14	3570.471120	18/07/2005	0.55598	227	15
1471.364134	19/10/1999	0.50805	103	14	3570.607966	19/07/2005	0.65834	325	20
1471.374810	19/10/1999	0.51603	120	14	3571.386693	19/07/2005	0.24079	265	30
1472.322382	20/10/1999	0.22478	199	20	3571.518360	20/07/2005	0.33927	265	15
1472.337247	20/10/1999	0.23590	190	20	3571.707795	20/07/2005	0.48096	155	20
1473.319694	21/10/1999	0.97073	196	18	3574.487220	22/07/2005	0.55986	288	15
1473.333869	21/10/1999	0.98133	208	20	3574.634575	23/07/2005	0.67008	244	15
1475.324003	23/10/1999	0.46987	183	20	3577.412992	25/07/2005	0.74822	269	15
1475.338872	23/10/1999	0.48099	164	20	3577.561738	26/07/2005	0.85948	241	15

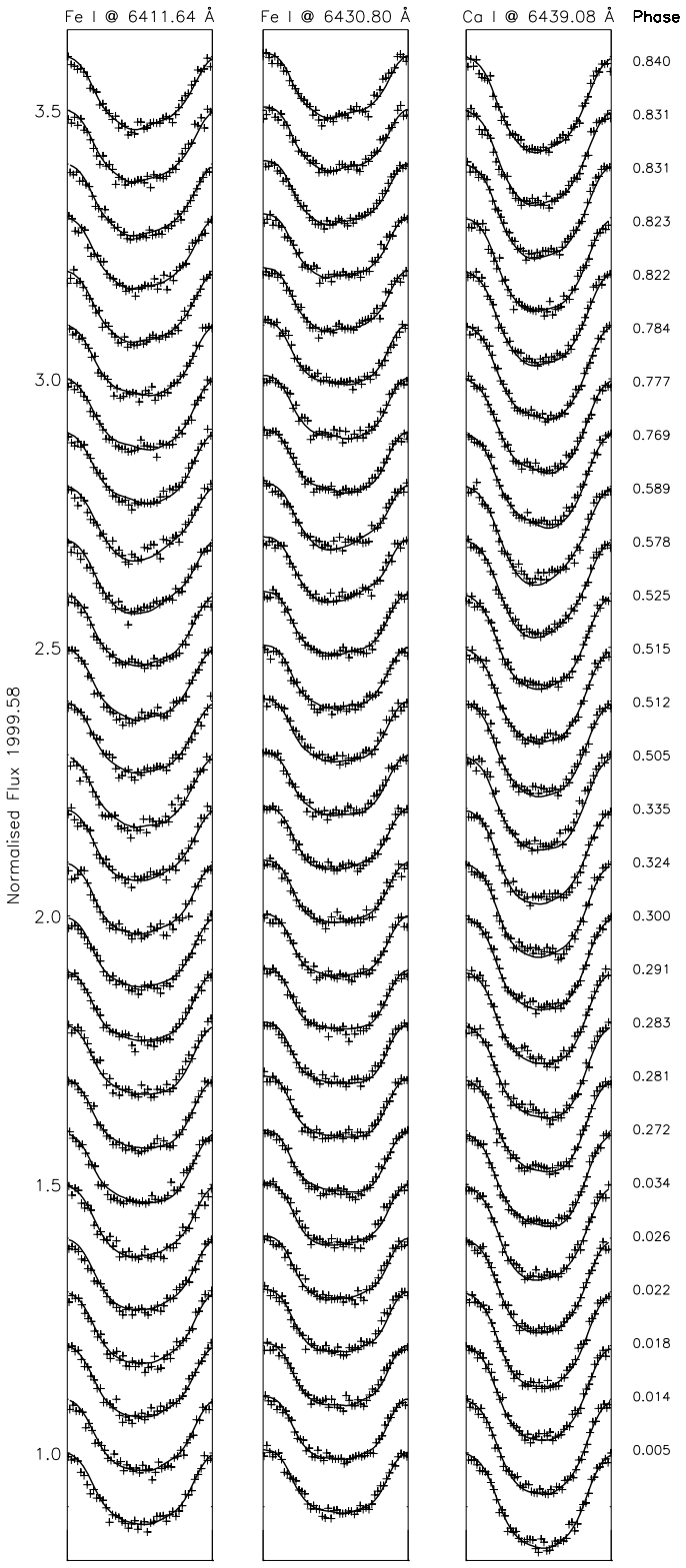

Fig. 7. Calculated (solid curves) and observed (crosses) spectral line profiles for the 1999.58 data set.

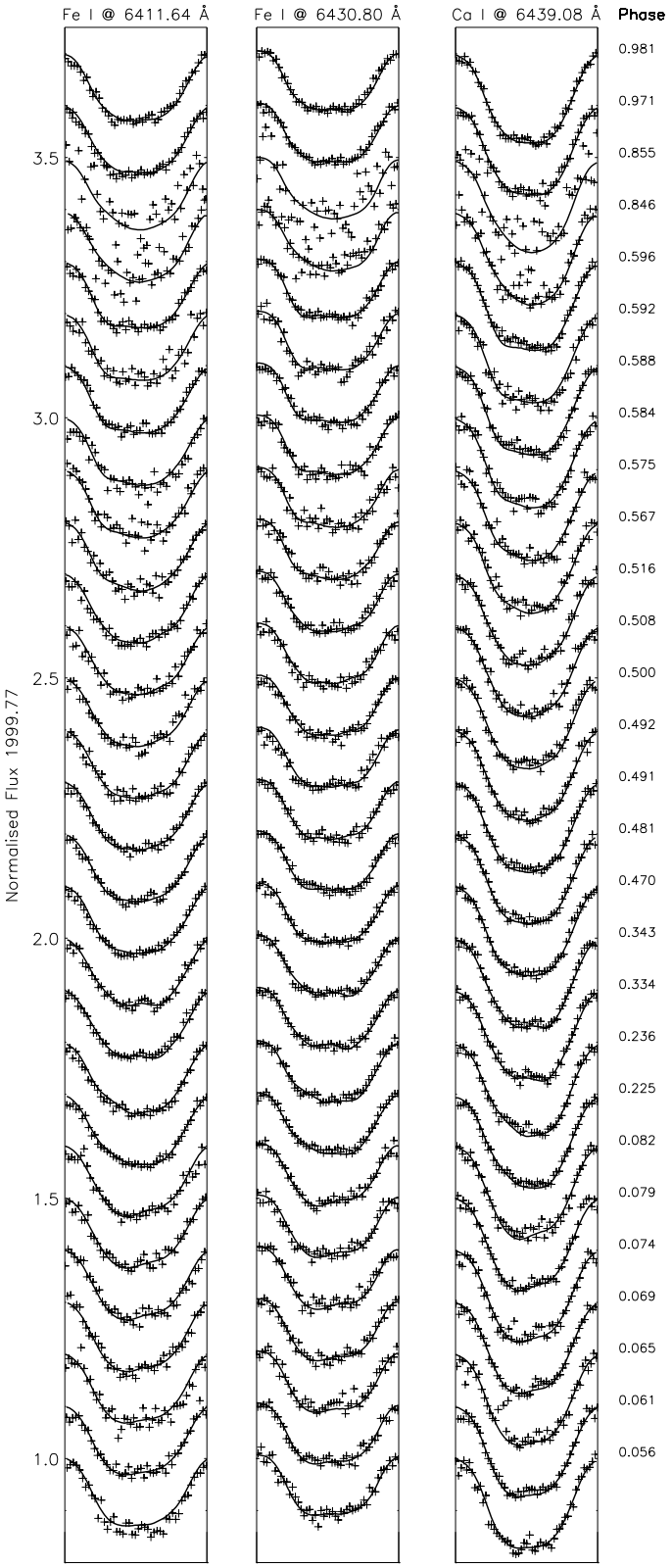

Fig. 8. The same as Fig. 7 but for the 1999.77 data set.

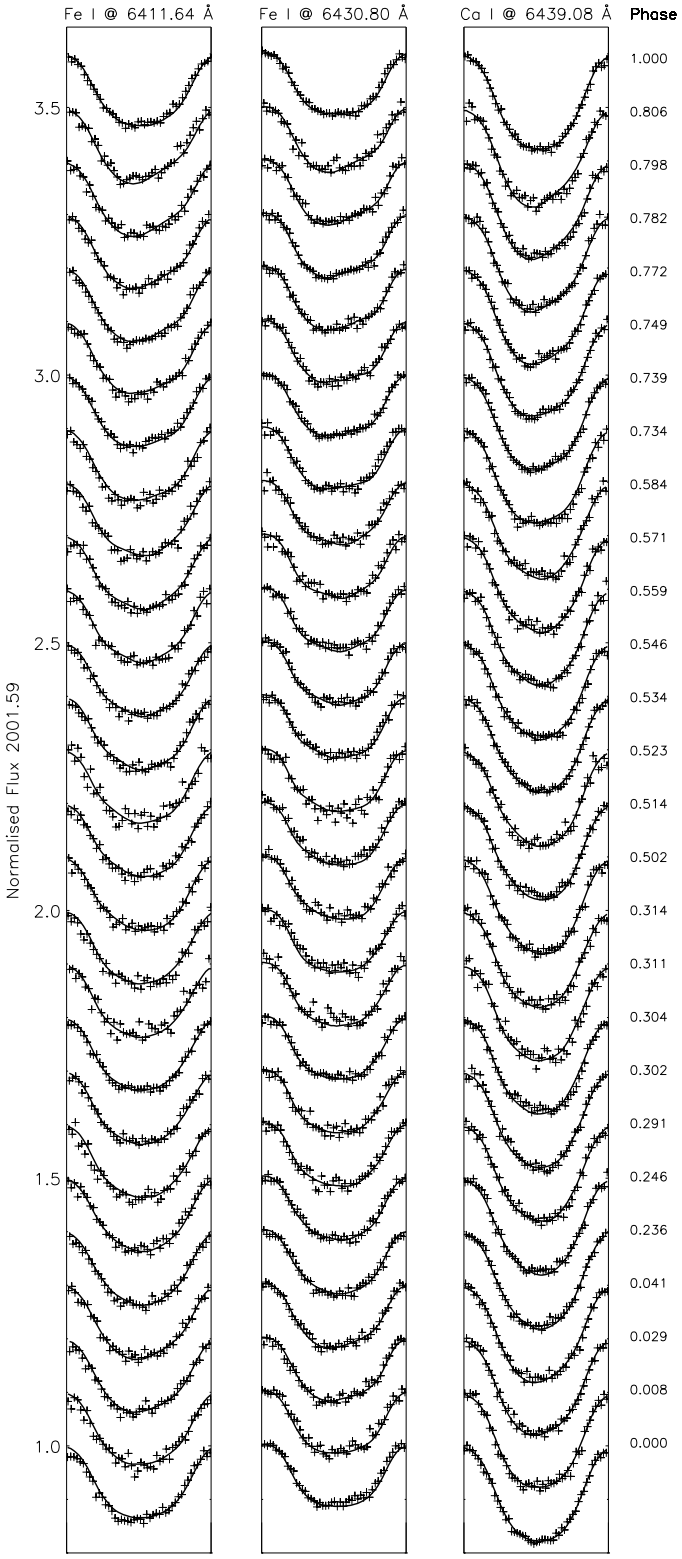

Fig. 9. The same as Fig. 7 but for the 2001.59 data set.

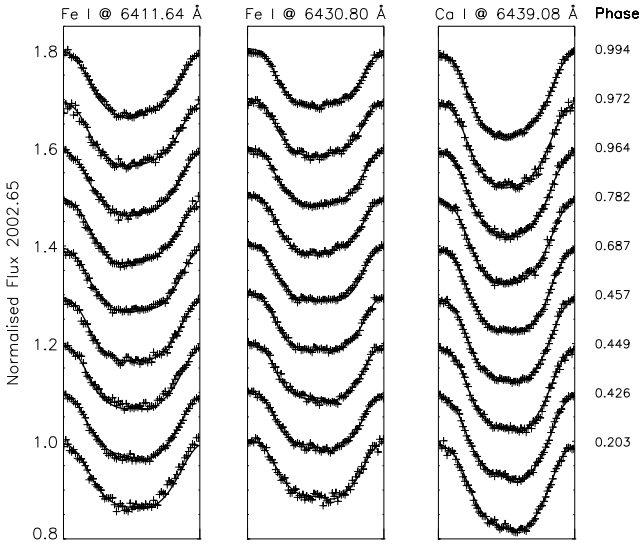

Fig. 10. The same as Fig. 7 but for the 2002.65 data set.

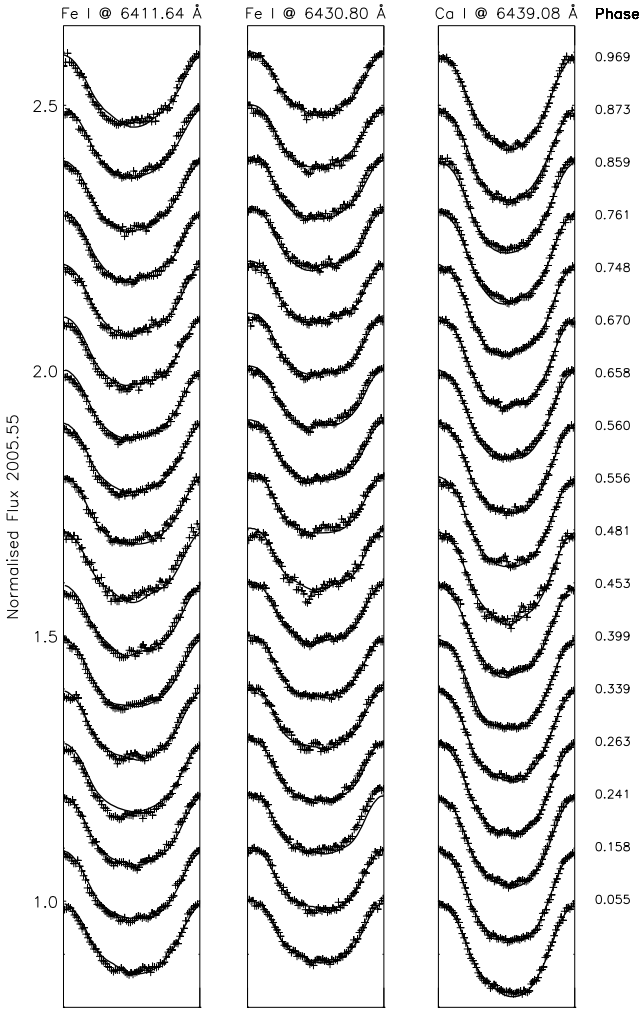

Fig. 11. The same as Fig. 7 but for the 2005.55 data set.